Dysregulated myeloid differentiation in colitis is induced by inflammatory osteoclasts in a TNFα-dependent manner

Maria Bernadette Madel, Lidia Ibáñez, Thomas Ciucci, Julia Halper, Antoine Boutin, Ghada Beldi, Alice C. Lavanant, Henri-Jean Garchon, M Rouleau, Christopher G. Mueller, et al.

Mucosal Immunology xxx (xxxx) xxx

Contents lists available at ScienceDirect

Mucosal Immunology

journal homepage: www.elsevier.com/mi

Dysregulated myeloid differentiation in colitis is induced by inflammatory osteoclasts in a TNFα-dependent manner

Maria-Bernadette Madel [a,2], Lidia Ibáñez [a,1,2], Thomas Ciucci [b], Julia Halper [a], Antoine Boutin [a], Ghada Beldi [a], Alice C. Lavanant [d], Henri-Jean Garchon [c], Matthieu Rouleau [a], Christopher G. Mueller [d], Laurent Peyrin-Biroulet [e,f], David Moulin [g,h], Claudine Blin-Wakkach [a,2,*], Abdelilah Wakkach [a,2,*]

[a] Université Côte d'Azur, CNRS, LP2M, Nice, France
[b] David H. Smith Center for Vaccine Biology and Immunology, Department of Microbiology and Immunology, University of Rochester Medical Center, Rochester, NY 14642, USA
[c] Université Paris-Saclay, UVSQ, INSERM, Infection et inflammation, 78180 Montigny-Le-Bretonneux, France
[d] CNRS UPR 3572, IBMC, University of Strasbourg, 67000 Strasbourg, France
[e] Department of Gastroenterology, IHU INFINY, CHRU Nancy, F-54500 Vandœuvre-lès-Nancy, France
[f] Université de Lorraine, INSERM, NGERE, F-54500 Vandoeuvre les Nancy, France
[g] Université de Lorraine, CNRS, IMoPA, F-54500 Vandœuvre Les Nancy, France
[h] IHU INFINY, Contrat d'interface, CHRU Nancy, France

ARTICLE INFO

Keywords:
Inflammatory bowel disease
Osteoporosis
Osteoclast
Myeloid progenitor cells
TNF-a

ABSTRACT

Inflammatory bowel disease (IBD) is characterized by very severe intestinal inflammation associated with extra-intestinal manifestations. One of the most critical ones is bone destruction, which remains a major cause of morbidity and a risk factor for osteopenia and osteoporosis in IBD patients. In various mouse models of IBD, we and other have demonstrated concomitant bone loss due to a significant increase in osteoclast activity. Besides bone resorption, osteoclasts are known to control hematopoietic niches in vivo and modulate inflammatory responses in vitro, suggesting they may participate in chronic inflammation in vivo. Here, using different models of colitis, we showed that osteoclast inhibition significantly reduced disease severity and that induction of osteoclast differentiation by RANKL contributed to disease worsening. Our results demonstrate a direct link between osteoclast activity and myeloid cell accumulation in the intestine during colitis. RNAseq analysis of osteoclasts from colitic mice revealed overexpression of genes involved in the remodeling of hematopoietic stem cell niches. We also demonstrated that osteoclasts induced hematopoietic progenitor proliferation accompanied by a myeloid skewing in the early phases of colitis, which was confirmed in a model of RANKL-induced osteoclastogenesis. Mechanistically, inhibition of TNF-α reduced the induction of myeloid skewing by OCL both in vitro and in vivo. Lastly, we observed that osteoclastic activity and the proportion of myeloid cells in the blood are positively correlated in patients with Crohn's disease. Collectively, our results shed light on a new role of osteoclasts in colitis in vivo, demonstrating they exert their colitogenic activity through an early action on hematopoiesis, leading to an increase in myelopoiesis sustaining gut inflammation.

Introduction

Inflammatory bowel disease (IBD), including Crohn's disease and ulcerative colitis, is a severe inflammatory disorder of the gastrointestinal tract with increased incidence of bone destruction, ranging from osteopenia to osteoporosis.[1–2] Bone destruction is a common complication in patients with IBD representing a major cause of morbidity and due to an over-activation of the bone resorbing OCLs. In this context, we identified $CD4^+$ Th17 as an osteoclastogenic subset emerging in IBD that induces OCL differentiation and links bone destruction to chronic

* Corresponding authors at: LP2M, Faculté de médecine, 28 Avenue de Valombrose 06107 Nice Cedex 2, France.
E-mail addresses: Blin@unice.fr (C. Blin-Wakkach), wakkach@unice.fr (A. Wakkach).
[1] Current address: Department of Pharmacy, Cardenal Herrera-CEU University, Valencia, Spain.
[2] Authors contributed equally to work.

https://doi.org/10.1016/j.mucimm.2024.09.005
Received 27 October 2023; Accepted 24 September 2024
Available online 26 September 2024

intestinal inflammation both in mice and patients.[3] However, the link between gut inflammation and OCL activity is not yet fully understood, particularly in view of the recent in vitro characterization of the immune function of OCLs,[4] especially in the context of IBD.[5] Indeed, OCLs are myeloid cells, and as such, emerging evidences reveal that they play a much broader role than bone resorption.[4] We and others demonstrated that OCLs are antigen-presenting cells that trigger immune tolerance in steady state.[5–7] Interestingly, we showed in vitro in the context of colitis that OCLs lose their tolerogenic capacity and instead display inflammatory properties associated with higher TNF-α expression compared to tolerogenic OCLs.[5] Altogether, these data revealed that OCLs are phenotypically and functionally heterogeneous depending on their context and may participate in the control of immune responses.[4]

Interactions between OCLs and osteoblasts are essential for bone remodeling, and are carried out in close proximity to hematopoietic stem cell (HSC) niches.[8–10] We previously showed that OCLs promote the formation of HSC niches at birth and modulate niches for B lymphopoiesis by controlling the fate of mesenchymal stromal cells (MSCs) that participate in these niches.[11–13] On the other hand, OCL formation is induced in response to acute stress signals or stimulation by RANKL (the main osteoclastogenic cytokine) and these OCLs secrete more proteolytic enzymes such as Matrix metallopeptidase 9 (Mmp9) and Cathepsin-K (Ctsk) that are involved in the remodeling of the niches and the mobilization of HSCs.[14] Furthermore, in steady state, in vivo blockade of OCL function reduces the number of HSC in the bone marrow.[15] Overall, these observations underline the fundamental role of OCLs in the regulation of hematopoiesis in response to acute stress, but which has not yet been investigated in the context of chronic inflammation. Interestingly, increased HSC proliferation and skewing towards myelopoiesis have been observed in chronic inflammation such as arthritis and colitis[16–18] where increased activation of OCLs has also been observed. Thus, participation of OCLs to HSC reactivation and myeloid skewing might represent an essential mechanism for initiating and sustaining chronic inflammation, which has been neglected and remains to be elucidated.

Here, to address the contribution of OCLs in the chronic inflammation and myeloid skewing observed in IBD, we used two well characterized and widespread models of colitis (Rag1-/- mice transferred with naive $CD4^+$ T cells, and WT mice treated with 3 % DSS). We showed that inhibition of OCL significantly reduced chronic colitis and that induction of OCL differentiation by RANKL contributed to worsening of colitis in both models. Our results showed a direct link between OCL activity and myeloid cell accumulation in the intestine during inflammation. Interestingly, we found OCLs to be activated very early during the disease. Bulk RNAseq analysis of colitic OCLs revealed an overexpression of genes involved in remodeling of HSC niches compared to control OCLs. We demonstrated for the first time that OCLs induce hematopoietic progenitor proliferation accompanied by a substantial myeloid skewing in the early phases of colitis. These results were further confirmed in the RANKL-inducing OCL model.

Mechanistically TNF-α blockade inhibited the induction of myelopoiesis by OCLs both in vitro in colony forming assays and in vivo in colitic mice, revealing that TNF-α is a major mediator of the induction of myeloid skewing by OCLs. Lastly, we observed an increase in myeloid cells correlated with high OCL activity in Crohn's disease patients.

Altogether, these data identify OCLs as potent regulators of HSC homeostasis and myelopoiesis required to maintain gut inflammation and point to them as a promising target in chronic intestinal inflammation.

Results

OCLs control intestinal inflammation

Since mouse models with inactive OCLs die before 3 weeks of age due to their severe osteopetrosis phenotype associated with strong hematopoietic defects in the BM,[11,19] we favored the use of pharmacological inhibitors used clinically to inhibit OCLs in osteoporosis. Thus, to assess the contribution of OCL activity in the development of intestinal inflammation, we used the well-characterized colitis model induced by transfer of naive $CD4^+CD45RB^{high}$ T cells into syngenic $Rag1^{-/-}$ mice.[20–22] These mice were treated with two anti-osteoclastogenic agents, the bisphosphonate zoledronic acid (ZA), and Calcitonin (Calci) that inhibit OCL formation and activity.[23] Treatment with both drugs one week after T cell transfer prevented colitis as assessed by reduced weight loss, clinical score and myeloid infiltration in the gut (Fig. 1A-D) and reduced OCL differentiation as indicated in Fig. 1E.

To confirm these results, we treated naive CD4 T cells-transferred $Rag1^{-/-}$ mice (referred to as colitic mice) with RANKL by i.p injection. RANK-L injection in mice is known to induce fast osteoclastogenesis in 2 days as shown in Suppl Fig. 1 A-B.[14,24] Our results show that colitic mice treated with RANKL developed a more severe colitis (Fig. 1 E-F) accompanied by an increased infiltration of monocytes and neutrophils in the lamina propria of the gut (Figure G-H) compared to untreated transferred mice. These results suggest that RANKL-induced osteoclastogenesis accelerates the development of colitis associated with highly increased number of monocytes and neutrophils in the gut.

To further validate the impact of OCLs on colitis in wild type mice, we exposed C57Bl/6 mice to Dextran Sodium Sulfate (DSS) in the presence or absence of RANKL as an alternative way of triggering colitis. C57Bl/6 mice that received RANKL by i.p injection and were sacrificed 2 days after, showed a marked decrease in femoral trabecular BV/TV attested by μCT and increase of OCL differentiation (Suppl Fig. 1A-B). Then, RANKL-treated C57Bl/6 mice were given 3 days of 3 % (w/v) DSS in drinking water and 4 days water as final cycle before euthanasia as indicated in Fig. 2A. Colitis-induced macroscopic changes (body weight loss, diarrhea, length of colon and size of spleen) were significantly exacerbated in RANKL treated mice compared with PBS-control mice (Fig. 2 A, B and C). The analysis of myeloid cell subpopulations in the lamina propria showed an increased infiltration of monocytes and activated macrophages in RANKL-treated mice (Fig. 2D-E). In contrast, C57Bl/6 mice treated with RANKL alone did not develop any signs of inflammation in the colon and we did not observe any activation of CD4 T lymphocytes or DCs, nor any expansion of innate lymphoid cells (ILCs) in particular ILC3 (Suppl Fig. 2A-F). These observations indicate that stimulation of OCL activity by RANKL aggravated DSS-induced colitis. Together, these findings suggest that OCLs control intestinal inflammation by exacerbating myeloid differentiation in the bone marrow.

Comparative transcriptomic analysis revealed that OCLs in colitis are distinct from control OCLs

To better understand the biological properties of OCLs in colitis, we performed transcriptomic profiling by bulk RNA-seq on mature multinucleated OCLs differentiated from the bone marrow (BM) of colitic mice (Rag 1-/- mice transferred with naive T cells) and of control Rag1-/- mice and sorted based on multinucleation as described.[25] A total of 453 genes were significantly differentially expressed ($pVal < 0.05$, $Log_2FC>1$) between the 2 populations. Interestingly, Principal Component Analysis (PCA) revealed that colitic and control OCLs were clustered into 2 distinct populations (Fig. 3A), which was reinforced by hierarchical clustering analysis (HeatMap) of the top of 60 significantly differentially expressed genes ($pVal < 0.05$, $Log_2FC>2$) (Fig. 3B). These results clearly demonstrate that colitic OCLs differ from control OCLs, confirming thereby the diversity of OCLs.[4] Pathway annotation using Gene Ontology Biological Process (GOBP, ShinnyGo) revealed strong association with inflammatory responses, various immune processes, and hemopoiesis (Fig. 3C) which was confirmed by gene set enrichment analysis (GSEA) on GOBP pathways for inflammatory response and cytokine production (Fig. 3D) confirming the differences previously observed in immune responses between control and colitic OCLs.[5] Moreover, pathway analysis also revealed association with OCL

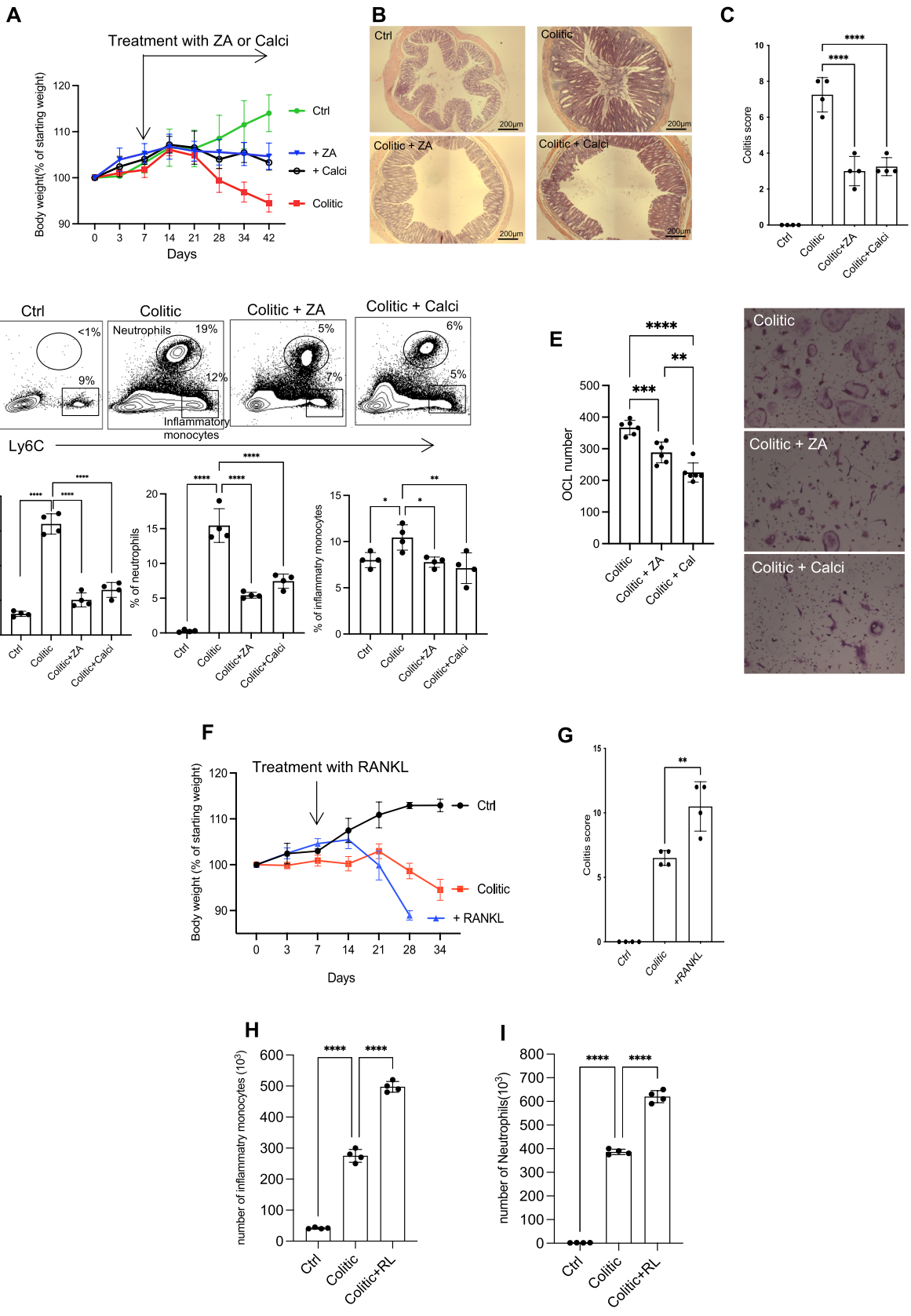

(caption on next page)

Fig. 1. Blockade of OCLs in the IBD model induced in *Rag1-/-* mice by naive CD4 T cell transfer reduces intestinal inflammation. (A) Naive CD4 + T cells transferred *Rag1-/-* mice were injected twice a week with zoledronic acid (ZA), Calcitonin (Calci) or PBS 1X (colitic), starting from week 1 (arrow "treatment"). The graph represents the mean weight normalized to the initial weight of each mouse of 4 animals per group, versus time. (B) Histological analysis of the distal colon from each mice group. Representative sets of H&E stained colonic sections from the indicated groups are shown. (C) Clinical score determined at 6 weeks of treatment. (D) Representative flow cytometry plot and percentage of neutrophils and monocytes in the colon. Histograms represent the mean ± SD of the indicated cells for 4 mice per group. (E) BM cells from treated with OCL inhibitors were differentiated in vitro into OCL as previously described.[25] OCLs were enumerated as TRAcP+cells with at least 3 nuclei. (F) Naive CD4 T cell-transferred *Rag1-/-* mice were injected with RANKL or PBS 1X (colitic), starting from week 1 (arrow "treatment"). The graph shows the weight of the mice (normalized to day 0) versus time. (G) Clinical score (mean ± SD) of the mice in each group. (H and I) Enumeration (the mean ± SD) of inflammatory monocytes and neutrophils in the colon of the mice (4 per group) in each group. All results are representative of data generated in at least three independent experiments. *p < 0.05; **p < 0.01; ***p < 0.001; ****p < 0.0001.

differentiation and tissue remodeling (Fig. 3C). In particular, colitic OCLs expressed higher levels of genes involved in OCL differentiation and bone resorption function, such as *Ctsk* and *Acp5*, 2 major enzymes involved in bone resorption, *Tcirg1* and *Clcn7* involved in mineralized matrix dissolution, *Nfatc1*, the master gene of OCL differentiation, and several metallopeptidases (Fig. 3E-F). This result is in line with the increased bone resorption previously observed in colitic mice.[3] Of note, among these genes, *Mmp9, Mmp14,* and *Ctsk* have been involved in HSC mobilization and expansion through their capacity to degrade HSC niche components.[26–27] Therefore, colitis OCLs generated from BM precursors in vitro differ from control OCLs, particularly in the expression of genes involved in bone resorption and HSC mobilization.

Increased OCL differentiation precedes the development of colitis

To better assess the contribution of OCLs to colitis, in particular, in the early stage of intestinal inflammation, we analyzed the number of OCLs during the first weeks after naive $CD4^+$ T cell-transfer and before any clinical signs are observed. As expected, during the first 3 weeks, transferred mice did not develop colitis as indicated by an increased body weight, the absence of clinical features of colitis and a clinical score below 2 (Fig. 4A). However, already by 3 weeks, the number of $TRAcP^+$ OCLs at the bone surface was considerably increased in the femur of colitic mice compared to controls (Fig. 4B-C). These results indicate that activation of OCL differentiation occurs before the clinical onset of colitis in these mice.

We then analyzed the expression of *Mmp9, Mmp14 and Ctsk* by RT-qPCR on purified OCLs derived from the BM of colitic mice at 2, 3 and 4 weeks. Our results clearly showed a significant increase of the expression of these 3 genes as early as week 2 after the induction of colitis. This increase peaked at week 3 with a 10-fold induction for *Mmp9* and *Mmp14* and a 3-fold induction for *Ctsk* (Fig. 4D). These results are consistent with the increased number of OCLs observed at 3 weeks.

Collectively, these data show that, contrasting with the common idea of late OCL activation as a consequence of inflammation, modifications in the number and phenotype of OCLs occur in the early stages of colitis.

Increase in HSC expansion and myeloid skewing in the BM of colitic mice

These results prompted us to analyze the influence of colitic OCLs on hematopoiesis and myelopoiesis. To address this point, we analyzed the hematopoietic Lin^- $Sca1^+$ $c\text{-}kit^+$ (LSK) progenitor cells in the BM of T cell-transferred mice during the first weeks. We observed an increase in the proportion of LSK cells as early as 2 weeks after transfer that continued to grow up to 15-fold at 3 weeks (Fig. 5A-C). This accumulation of LSK cells is associated with an increase of their proliferation attested by Ki-67 staining (Fig. 5D). These results suggested an alteration of the niche generally linked to LSK cell mobilization, which was confirmed by their increased proportion in the spleen of T cell-transferred mice compared to controls (Suppl Fig. 2A-B). Overall, LSK cell proliferation was increased in the BM of T-cell-transferred mice, which was particularly striking at week 3 in parallel with the increased osteoclastogenesis.

To determine whether the activation of HSC progenitor cells might subsequently induce a change in the orientation of their differentiation, the proportion of common myeloid progenitor (CMP), megakaryocyte-erythrocyte progenitor (MEP) and granulocyte-monocytes progenitors (GMP) were quantified. During the first weeks after T cell transfer in *Rag1*$^{-/-}$ mice, the cell composition within the myeloid progenitor (MP) cells (Lin^{neg} $c\text{-}kit^{high}$ $Sca\text{-}1^{neg}$) changed considerably with a shift to increased GMP that peaked at week 3 compared to control mice (Fig. 5E-F). Altogether, the myeloid progenitor composition was dramatically altered with a skew toward GMP differentiation particularly at week 3. The consequence of this change was also observed in the periphery with extramedullary hematopoiesis in the spleen (Suppl Fig. 2A-B) as well as an accumulation of monocytes and neutrophils in the spleen of T cell transferred *Rag1*$^{-/-}$ mice (Suppl Fig. 2C-D).

Progenitor expansion and myeloid skewing are induced by colitic OCLs

We next confirmed the implication of OCL in this myeloid skewing in vivo by stimulating OCL formation by RANKL injection in C57Bl/6 mice as shown in Suppl Fig. 1. As expected and already described,[14] the number of $TRAcP^+$ OCLs on bone surface was elevated in treated mice compared to controls (data not shown). We also observed an increase in the percentage and absolute number of LSK cells (Fig. 6A-B), confirming the data previously reported.[14] Interestingly, we also observed a shift in hematopoiesis towards increased GMP formation in mice injected with RANKL (Fig. 6C-D), confirming that increased OCL formation is associated with myeloid skewing in vivo.

We next blocked RANKL-induced OCL formation in Rag1-/- mice transferred with naive T cells to evaluate the effect of OCLs on hematopoietic progenitor expansion in vivo. LSK cell and GMP percentages were significantly decreased in the BM of T cell transferred mice injected with anti-RANKL antibody compared to mice injected with an isotype control antibody (Fig. 6E-F). Furthermore, treatment with the 2 anti-osteoclastogenic agents (ZA and Calci) caused a significant decrease in the percentage of LSK cells and their proliferation (Fig. 6 G-I) as well as their differentiation towards GMP (Fig. 6J).

Collectively, these data showed a fundamental role of colitic OCLs in the proliferation and myeloid skewing of LSK cells, which could place OCL activity as a key downstream colitogenic mechanism leading to increase inflammatory myelopoiesis and colitis.

TNF-α promotes OCL-driven myeloid skewing

Hematopoiesis is tightly controlled by the interaction between hematopoietic progenitors and mesenchymal stromal cells (MSCs). To evaluate how OCLs can induce myeloid skewing from LSK cells, we performed colony-forming assay of sorted LSK cells, in co-culture with MSCs (BM $CD45^{neg}$ cells) from control mice and OCLs from colitic or control mice. Our results showed that the presence of purified colitic OCLs is sufficient to dramatically enhance the number of CFU-GM from LSK cells (Fig. 7A) compared to OCLs from control mice. Interestingly, in the absence of MSCs, OCLs don't have any effect on CFU-GM, indicating that they act by disrupting the interaction between LSK cells and their niche (MSCs) (Fig. 7A).

Our previous study showed that, compared to steady state OCLs, inflammatory OCLs express higher level of inflammatory cytokines including TNF-α.[5] To assess the effect of TNF-α on the myeloid skewing,

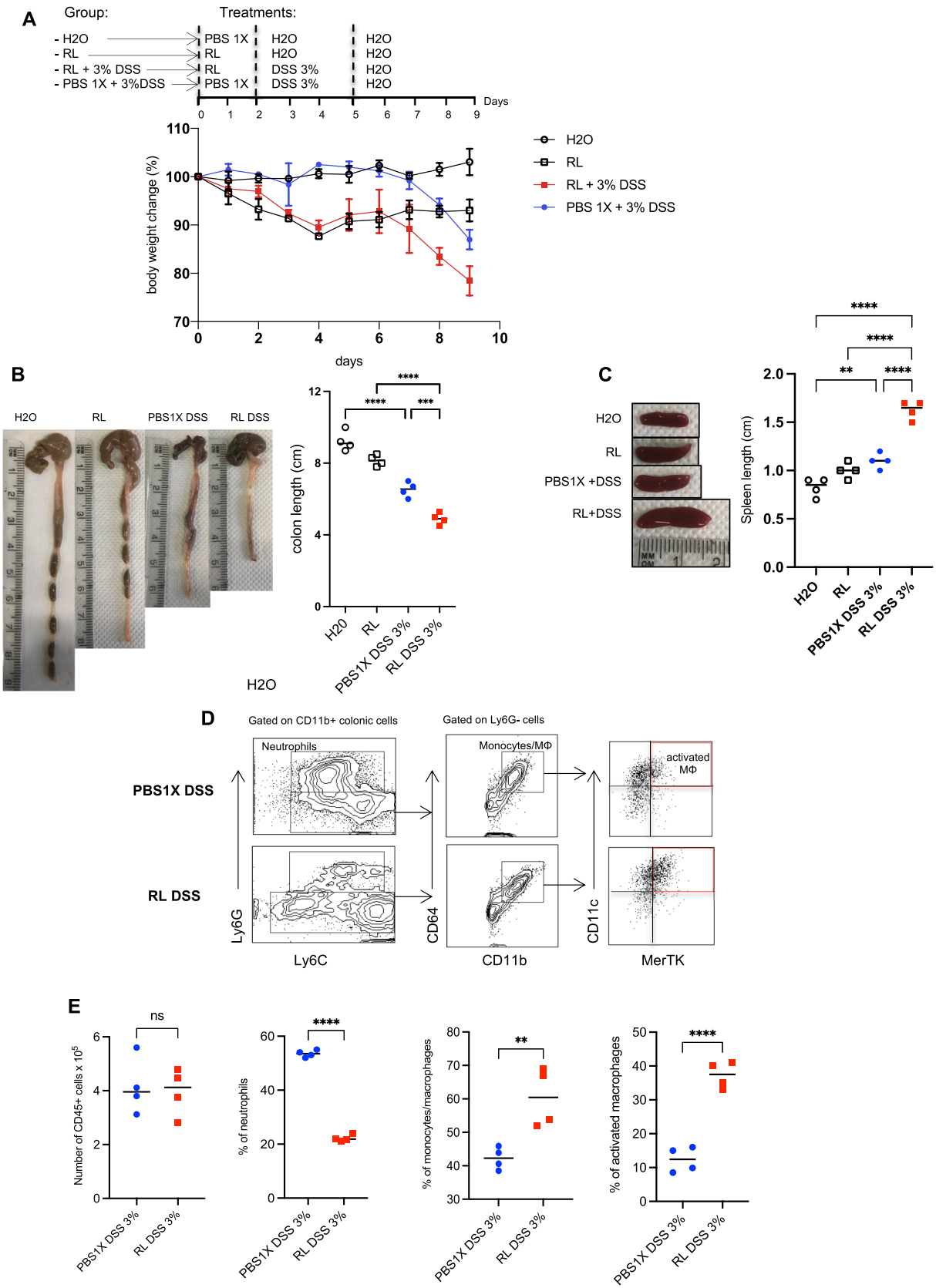

Fig. 2. Intestinal inflammation in DSS-colitis mouse model is accelerated after OCL induction by RANKL. (A) Daily recording of body weight during experiments. (B) Representative photos of colon length and quantitation of colon length. (C) Gross appearance of the spleen and quantitation of spleen length. (D) Representative staining of Neutrophils, monocytes and macrophages from the colon. Data are representative of two independent experiments. **p < 0.01; ****p < 0.0001.

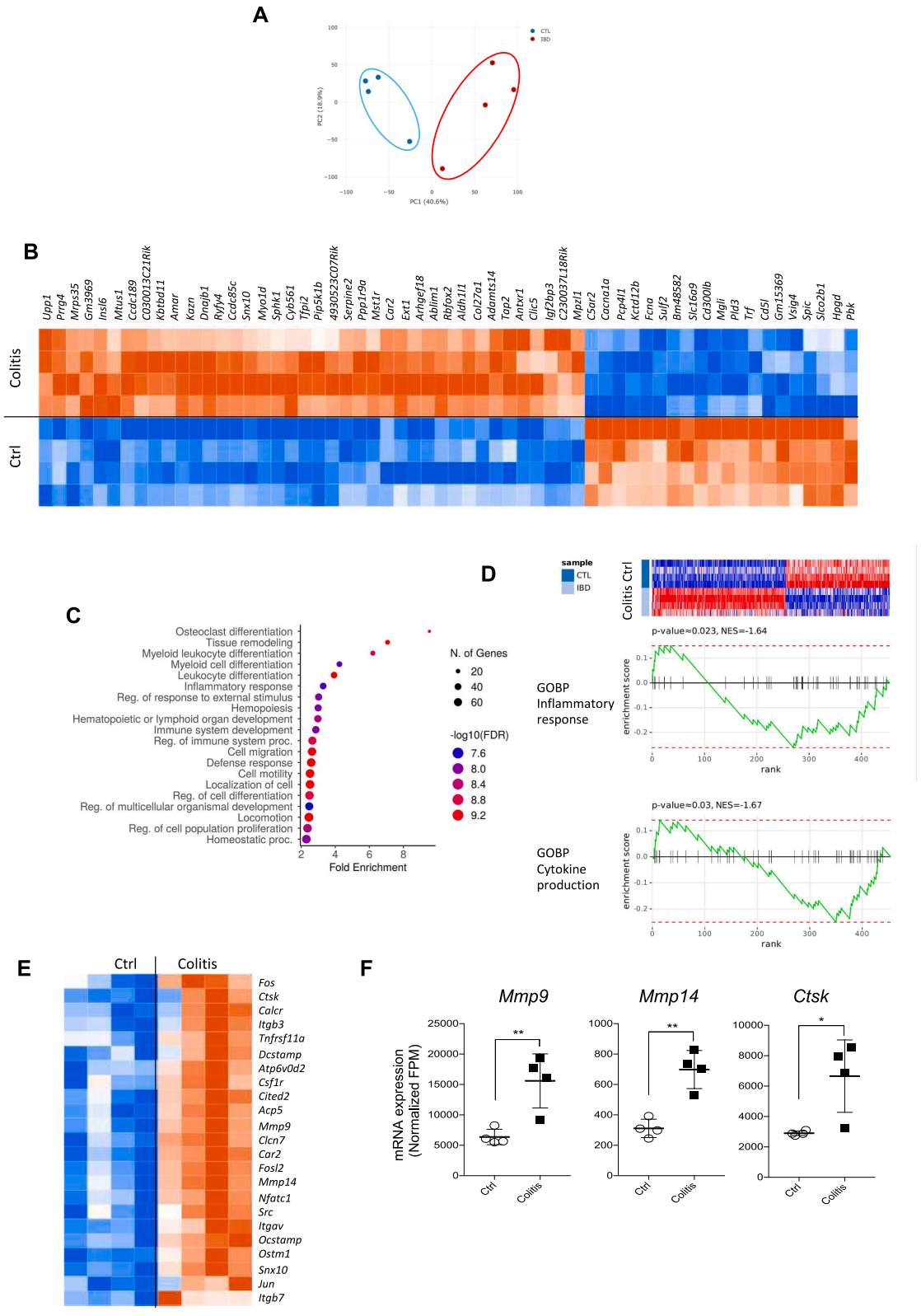

Fig. 3. Comparative analysis of purified OCLs from colitic and control mice revealed distinct transcriptomic signatures. Sorted mature OCLs generated from the bone marrow (BM) of colitic (6 weeks after T cell transfer) and control mice were compared using bulk RNAseq analysis. (A) Principal component analysis of the genes showed that colitic and control OCLs segregate into 2 distinct clusters. (B) Heatmap visualization of the top 60 differentially expressed (DE) genes (pVal < 0.05, $Log_2FC>1$). (C) Pathway annotation of the 453 DE genes with ShinnyGo using GO-Biological Process. (D) Gene set enrichment analysis (GSEA) on GOBP pathways for inflammatory response and cytokine production. (E) Heatmap visualization of selected genes involved in OCL differentiation and bone resorption activity that are significantly increased in colitic OCLs compared to control OCLs (pVal < 0.05). (F) Expression of *Mmp9*, *Mmp14* and *Ctsk* in colitic and control OCLs from the RNAseq analysis. Data are expressed as fragments per million (fpm) normalized to total reads per sample. *p < 0.05; **p < 0.01.

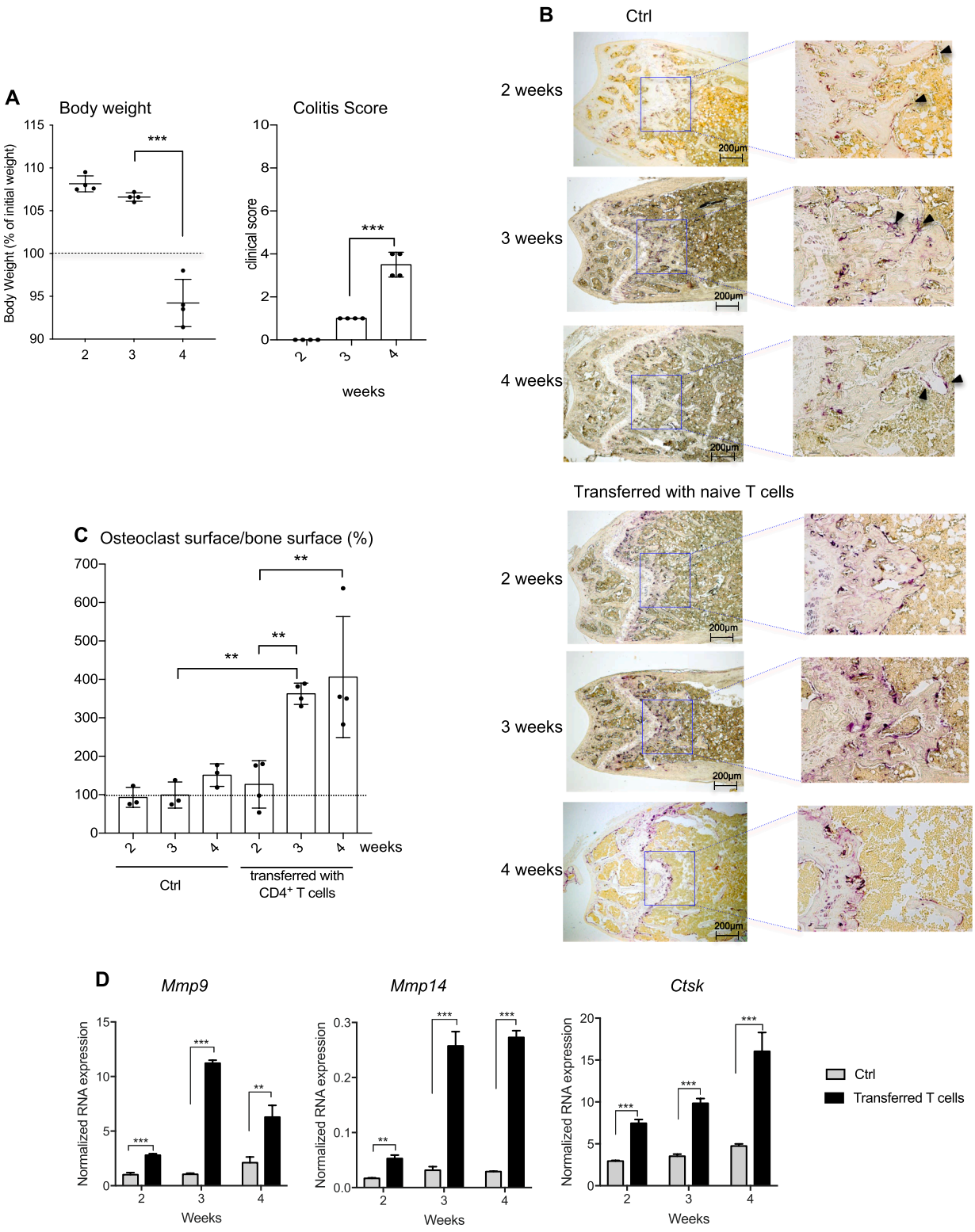

Fig. 4. Increased OCL differentiation precedes the development of colitis Rag1-/- mice received naive CD4 T cells (referred to as transferred mice) or PBS 1X (Ctrl) and were analyzed at the indicated time. (A) Clinical score of transferred *Rag 1-/-* mice. (B) TRAP staining of femora from controls and transferred *Rag 1-/-* mice. Arrowheads indicate TRAP^{+} OCLs. (C) Quantification of OCLs (TRAP+cells with 3 nuclei and more) at bone surface. (D) RT-qPCR analysis for the expression of *Mmp9*, *Mmp14* and *Ctsk* genes in colitic and control OCLs at week 2, 3 and 4 after transfer of naive CD4 T cells or PBS 1X injection. Results were normalized to the 36B4 gene. Data are representative of three independent experiments. *$p < 0.05$; **$p < 0.01$; ***$p < 0.001$.

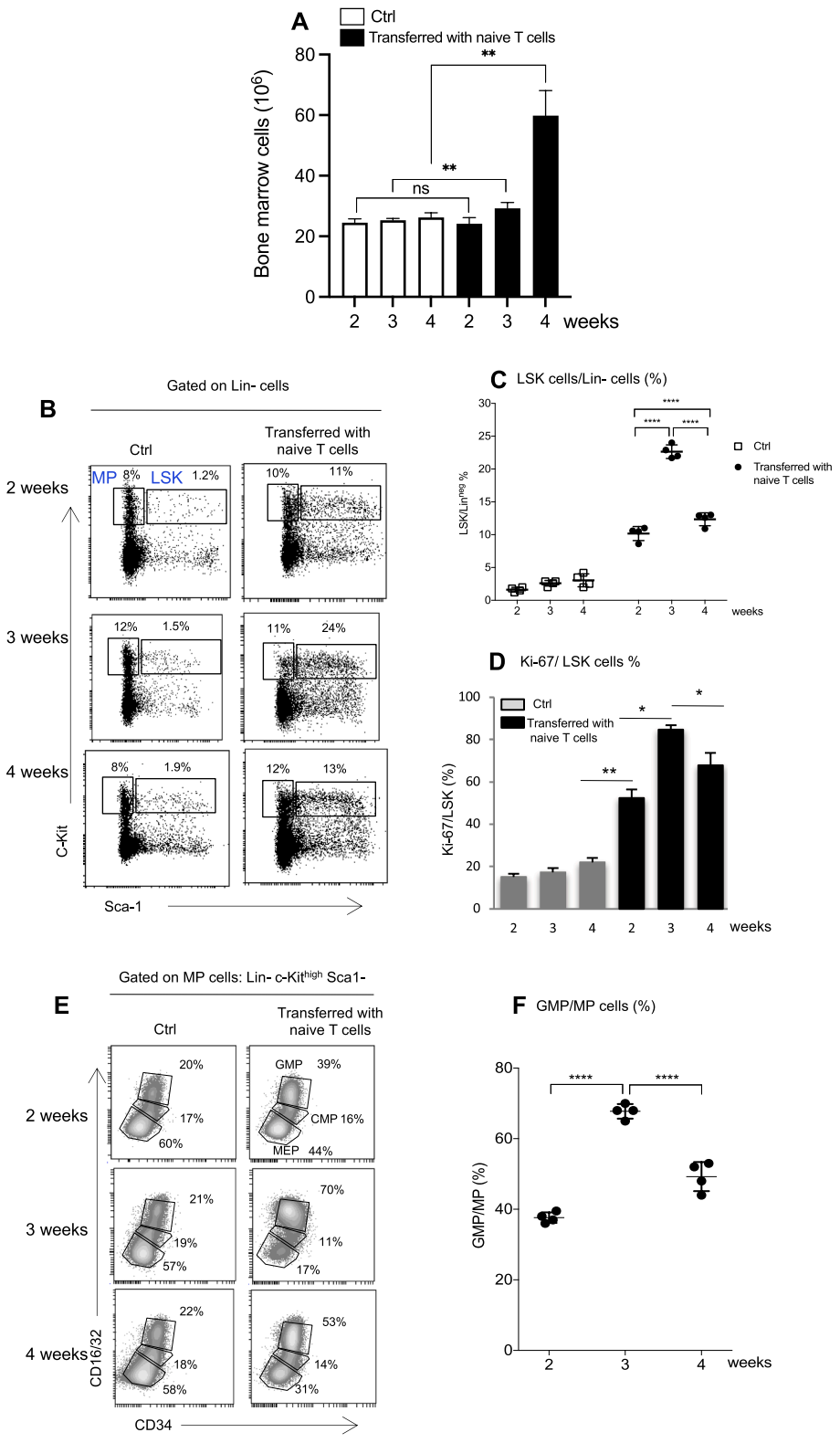

Fig. 5. Increased in HSC expansion and myeloid skewing in the BM of colitic mice. (A) Total cell numbers in BM (one leg, femur and tibia). (B) Representative flow cytometry staining of LSK cells. (C) Percentage of LSK cells among BM Lin$^-$ cells of control (Ctrl) and transferred *Rag1-/-* mice at different time as indicated. (D) BM cells were stained for the proliferation marker Ki-67 and the proportion of Ki-67 + cells among LSK cells was analyzed by flow cytometry. (E) Representative flow cytometry analysis of CMP, GMP and MEP progenitors in the BM. (F) Percentage of GMPs among of MPs. Each point represents an individual mouse. Data are representative of at least three independent experiments. *$p < 0.05$; **$p < 0.01$; ****$p < 0.0001$.

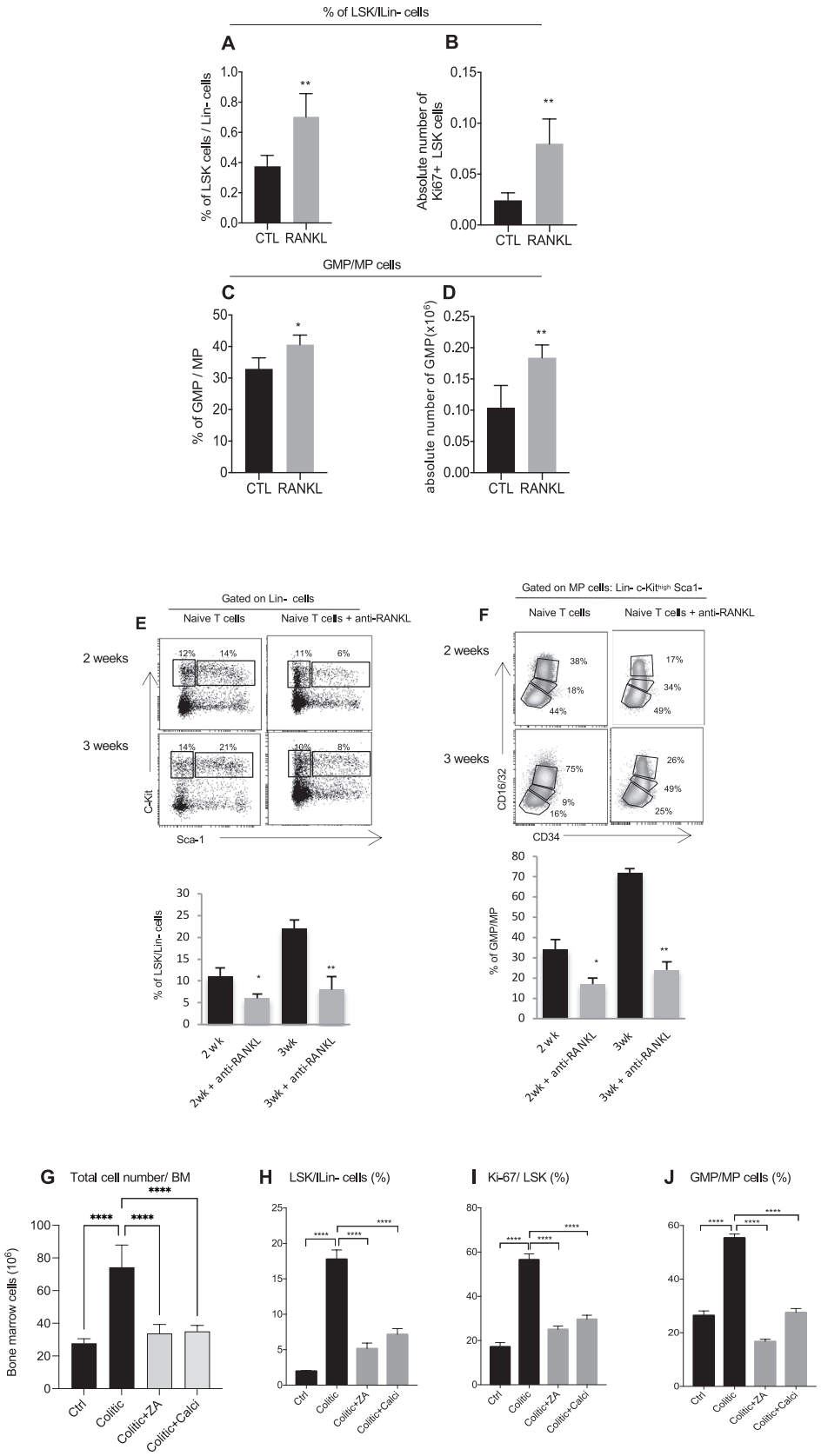

(caption on next page)

Fig. 6. Progenitor expansion and myeloid skewing are induced by colitic OCLs. Absolute numbers (A) and proliferation assessed by Ki-67 (B) of LSK cells in the BM of wild type mice injected with RANKL. (C-D) Percentages and absolute numbers of GMP in the BM of wild type mice injected with RANKL. Data are representative of two independent experiments. (E-F) *Rag1-/-* mice were injected 24 h after naive CD4 T cell transfer with anti-RANKL twice per week for 2 and 3 weeks. Representative flow cytometry analysis of LSKs (E) and and GMPs (F) in the BM of untreated and treated transferred *Rag1-/-* mice with RANKL. Data are representative of two independent experiments. *$p < 0.05$; **$p < 0.01$. Transferred *Rag1-/-* mice were injected twice per week with zoledronic acid (ZA), calcitonin (Cal) or PBS 1X (colitic), starting from week 1 as indicated in Fig. 1. (G-J) Absolute numbers, percentage, proliferation of LSKs and percentage of GMP population in the BM. All results are representative of data generated in three independent experiments. ****$p < 0.0001$.

we neutralized TNF-α in the co-culture. In fact, anti-TNF-α treatment induced a dramatic reduction of the number of CFU-GM in the presence of colitic OCLs (Fig. 7B). To further validate the role for TNF-α in promoting OCL- induced myeloid skewing, we used TNF-α KO mice to generate either MSC or inflammatory OCLs deficient in TNF-α and perform CFU-GM assays. Our results confirmed that WT inflammatory OCLs increased CFU-GM numbers, whereas those from TNF-α KO did not (Fig. 7C). Furthermore, the presence of BM MSCs from TNF-α KO mice did not affect CFU numbers, suggesting a role for a role for TNF-α in promoting OCL- induced myeloid skewing (Fig. 7C). Interestingly, the increase in CFU-GM was not observed when using inflammatory monocytes instead of inflammatory OCLs in coculture with MSC (data not shown). We next confirmed these results in vivo by anti-TNF-α injection into Rag1-/- mice transferred with naive T cells. Interestingly, treatment with anti-TNF-α showed a significant reduction in GMP as shown in Fig. 7D. Taken together, these findings suggest that OCLs participate in myeloid skewing of HSCs during colitis in a TNF-α dependent manner.

Increased in myeloid dendritic cells and pro-inflammatory monocytes in Crohn's disease patients correlates with high OCL activity

We next evaluated the link between OCL activity and myelopoiesis in patients affected with Crohn's disease (CD). Serum concentration of Cross laps (CTx), the carboxyterminal telopeptide region of type I collagen alpha (1) chain cleaved by OCLs during bone resorption, reflects the osteoclastic activity.[28] CTx levels measured in the serum of 6 patients with CD (recently diagnosed) and 6 healthy donors, were increased in the CD patients compared to controls (Fig. 8A). In parallel, we observed a significant increase in the percentage of myeloid BDCA-1^+ DCs in the blood of CD patients compared to the controls (Fig. 8B). In agreement with recent studies,[29–30] a significant increase of intermediate $CD14^+$ $CD16^+$ blood monocytes was also observed in patients with CD versus controls (Fig. 8C). We next asked whether this increase in inflammatory myeloid cells in CD disease correlated with OCL activity. In contrast to the non-classical monocytes, there was a strong correlation between CTx and the blood proportion of BDCA-1^+ DCs ($R^2 = 0.94$), as well as intermediate monocytes ($R^2 = 0.78$) (Fig. 8D-E). These data suggest that, as in mice, increased OCL activity in CD patients could potentially participate in increased myelopoiesis.

Discussion

Myeloid skewing is a hallmark of chronic inflammatory diseases and in particular inflammatory bowel disease. Despite their well described implication in the modulation of hematopoietic niches in acute stress, as well as their innate immune function, participation of OCLs in this dysregulated myelopoiesis remains neglected. Here, we show that OCLs are activated very early in colitis, before clinical signs of gut inflammation and are involved in the increased myelopoiesis observed in this context by disrupting interaction between HSCs and the MSCs forming their niches, in a TNF-α-dependent manner. Moreover, early blockade of OCL significantly reduces myelopoiesis. Therefore, these results revealed an unexplored function of OCLs in sustaining inflammation through the modulation of myelopoiesis.

Interestingly, transcriptomic profiling of colitic OCLs revealed an overexpression of genes involved in bone resorption in line with the high level of bone destruction observed in colitic mice and IBD patients.[2–3] We show that in vivo inhibition of OCL in colitic mice reduces the severity of the disease and the level of myelopoiesis, and in the other end that stimulating OCL activity in normal mice strongly enhances myelopoiesis. The implication of OCLs in the control of myelopoiesis is further demonstrated by our in vitro clonogenic assays in which the number of CFU-GM is dramatically augmented only in the presence of colitic OCL. Interestingly, transcript levels of *Mmp9*, *Mmp14* and *Ctsk*, encoding proteolytic enzymes known to induce mobilization of BM progenitors,[31–32] were increased during the first weeks before the onset of colitis. *Mmp9* and *Mmp14* expressed in OCLs jointly participate in bone resorption making them key regulators of OCL activity *in vivo*.[33] Furthermore, the activity of Mmp9 and Mmp14 disrupts major niche factors, such as CXCL12 and kit ligand (SCF) involved in HSC retention and homeostasis, which facilitates release and egress of HSCs.[27] Increased expression by colitic OCLs of the Mmp9/Mmp14 couple may represent a molecular mechanism by which the colitic OCLs induce the expansion of HSCs during the onset of colitis. In other hand, Ctsk, the key marker of bone degradation, also has an important role in the regulation of niche factors such as CXCL12, and in progenitor mobilization, together with Mmp9, in acute stress condition.[14] Overall, our results suggested that overexpression of Ctsk and Mmp9/Mmp14 in colitic OCLs, each with a variety of overlapping substrates involved in HSC niches, may contribute to the disruption of the interaction between HSCs and their niches, providing a powerful regulation of the niche and thus facilitating HSC mobilization and myeloid skewing observed early in the disease.

Importantly, we found OCLs to be activated very early, and before any gut inflammation is observed. OCL activation is generally considered as a late consequence of inflammation. However, several observations revealed that they may play a role in the inflammatory process. First, in inflammatory condition, OCLs as innate immune cells have a direct inflammatory role that has been demonstrated in vitro.[5] Moreover, clinical observations revealed that local and systemic bone loss is detected very early in the rheumatoid arthritis (RA) disease process. Indeed, It was shown that antibodies against citrullinated proteins (ACPA) bind OCL progenitors and directly promote their differentiation into OCLs and that, in ACPA positive patients, bone loss starts even before the onset of clinical disease.[34–35] Interestingly, our results in Crohn's patients prior to treatment showed an increase in the level of CTx in the blood indicating a high OCL activity. In addition, there was a strong correlation between CTx and the proportion of inflammatory myeloid cells. This result suggests that osteoclastic activity may also increase early during the human disease and accelerate throughout the years of the disease. This would promote an early HSC expansion with myeloid skewing leading to a destructive feed-forward loop in which increased numbers of inflammatory myeloid cells would enhance inflammatory cytokines, which in turn would perpetuate an aberrant hematopoiesis response and an increased osteoclastogenesis leading to osteoporosis. It would be interesting to extend the cohort of patients at the start of IBD to validate this hypothesis.

Inflammatory cytokines directly control distinct components of the aberrant hematopoietic response. In colitis, IFN-γ increases HSC proliferation and GM-CSF is involved in the accumulation of GMPs in the BM.[17] TNF-α is the most significantly increased cytokine across multiple murine models of IBD.[36] Interestingly, we show in our in vitro clonogenic assay that TNF-α blockade significantly reduced the increase in CFU-GM induced by colitic OCLs. These results suggest that OCLs participate in myeloid skewing of HSCs during colitis in a TNF-α

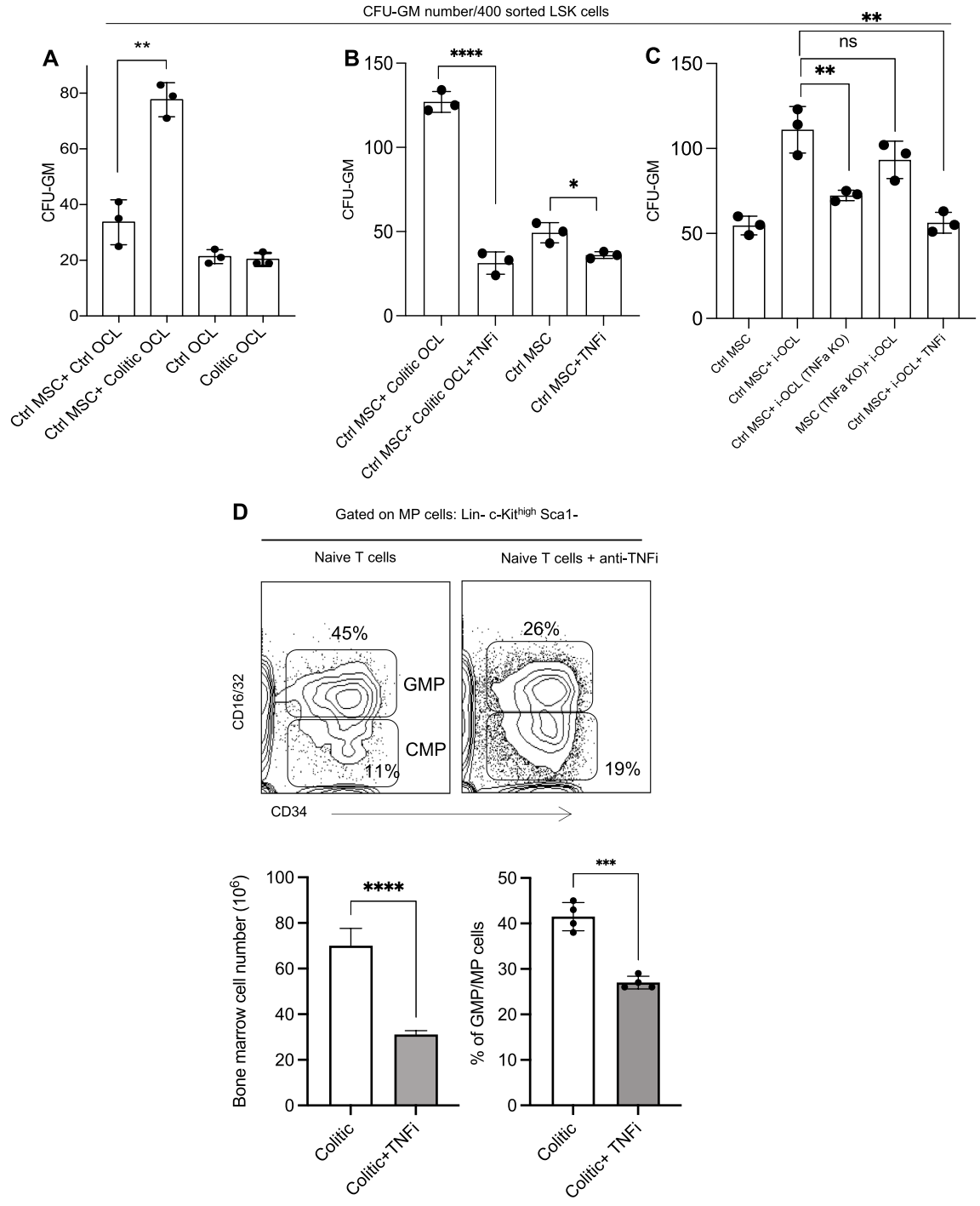

Fig. 7. OCL-derived TNFa promotes myeloid skewing Colony-forming assay (CFU-GM) of sorted LSK cells in co-culture with MSCs from the BM of control mice and in the presence of sorted OCLs differentiated from BM of colitic or control mice (A) or in presence of anti-TNF-α (B). (C) CFU-GM assay of sorted LSK cells in co-culture with MSC from the BM of control mice or from TNF-α KO mice and in the presence of sorted inflammatory OCLs (i-OCLs) from control mice or from TNF-α KO mice. The data are presented as the mean+/-SD of GM-CFU numbers induced by MethoCult GF 3434 medium. Each point represents the average of triplicate of each mouse. Data are representative of two independent experiments. *$p < 0.05$; **$p < 0.01$; ****$p < 0.0001$. (C) Naive CD4 T cells transferred *Rag1*-/- mice were injected twice per week with TNF-α inhibitor (Etanarcept), starting from week 1during 3 weeks. Percentage of GMP in the BM was analyzed by flow cytometry. Each point represents an individual mouse. Data are representative of two independent experiments. ***$p < 0.001$; ****$p < 0.0001$.

dependent manner.

Peripheral inflammatory myeloid cells have a major pathologic role by infiltrating the mucosa and contribute to the initiation and perpetuation of mucosal inflammation characteristic for human IBD. They are targets for interventions by ablation or granulocyte/monocyte apheresis (GMA) which led to major improvements in IBD therapy even in patients with CD refractory to conventional medications.[29,37–38] Anti-resorptive treatments such as bisphosphonates (ZA) are used to treat bone resorption in IBD patients developing osteoporosis.[39] As bone resorption is coupled with bone formation, these long-term treatments also inhibit bone remodeling and dramatically affect the bone quality, increasing the risk of fracture and osteonecrosis. In contrary to our observations, ZA

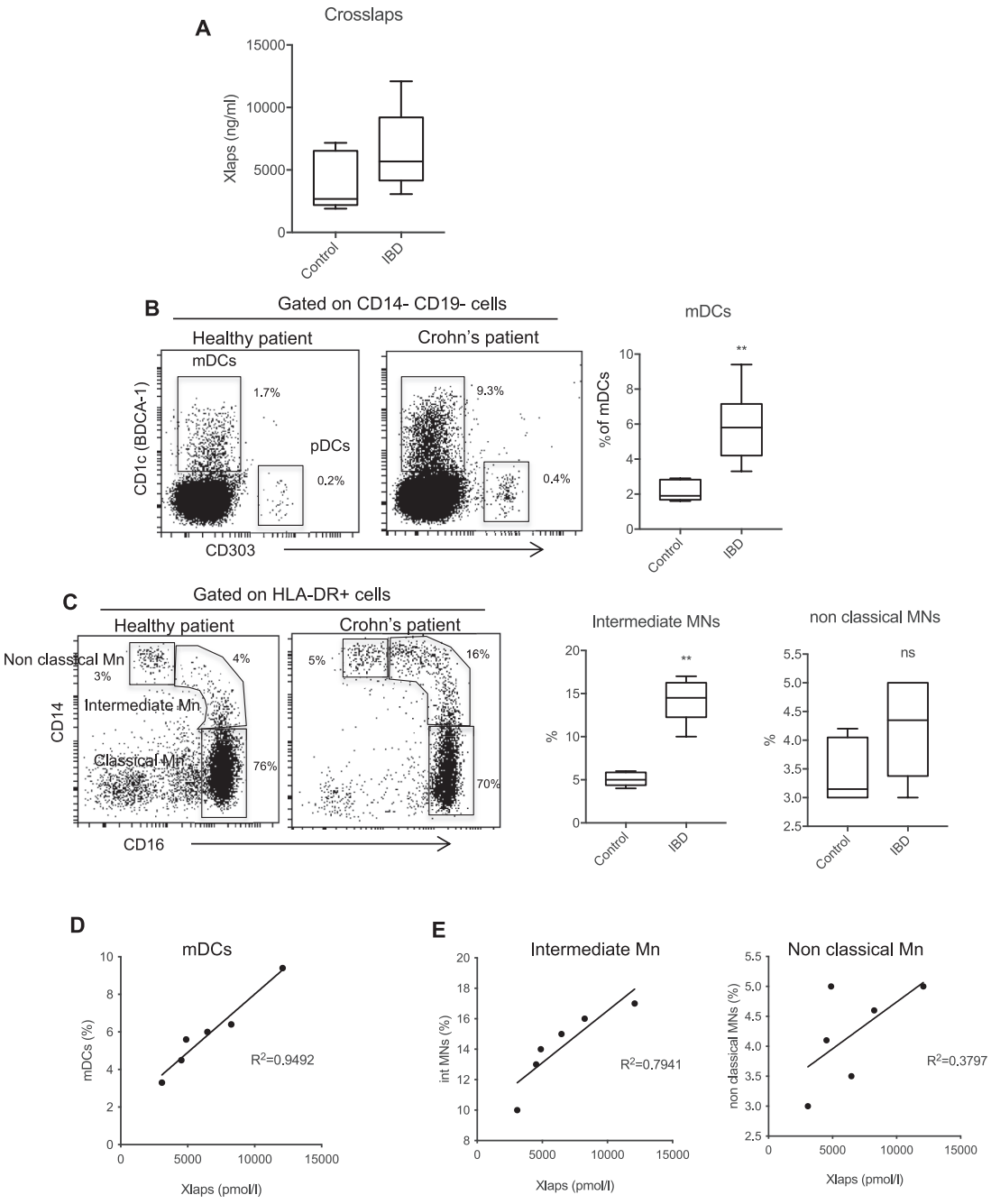

Fig. 8. Increase of myeloid dendritic cells and pro-inflammatory monocytes in Crohn's disease (CD) patients is correlated with OCL activity. (A) Serum concentration level of CTx in healthy donor and patients with CD. Frequency of dendritic cells (DCs) (B) and monocytes (Mn) (C) in the peripheral blood from healthy donor or patients with CD were assessed by flow cytometry. Correlation between CTx and myeloid DCs (D) or monocytes subsets (E) was analyzed using the spearman's rank correlation test.

promotes the accumulation of myeloid progenitors by blocking their differentiation into macrophages and dendritic cells in cancer context.[40–41] These controversial effects can probably be explained by differences in the models used.

Ultimately, we believe that precise characterization of OCLs that control the function of hematopoietic system will offer opportunities to develop novel therapeutics in IBD but also in other chronic inflammatory diseases with a strong myeloid component such as rheumatoid arthritis and spondylarthritis. It will also improve our general understanding of the implication of OCLs in the regulation of hematopoiesis.

Materials and methods

Mice

C57BL/6J mice were purchased from Harlan Laboratory (France), and C57BL/6 Rag1$^{-/-}$ mice from Charles River Laboratory (France). The TNF-α KO mice were kindly provided by Dr A Monfort (Cancer research center of Toulouse). Animals were maintained in our animal facility in accordance with the general guidelines of the institute, and approval for their use in this study was obtained from the Institutional Ethic Committee for Laboratory Animals (CIEPAL-Azur). Bone loss model with inflammatory OCLs was mimicked by i.p. injection of RANKL in C57BL/

6J mice as described in.[24]

Induction of colitis

Colitis was induced in Rag1$^{-/-}$ mice by one i.p. injection of 4.10^5 sorted splenic naive CD4$^+$CD25^{neg}CD45RB^{high} T cells from C57BL/6J mice as described.[22] When indicated, mice were i.p injected twice a week with 0.25 mg of anti-RANKL (IK22-5) or isotype control (rat IgG2a, eBioscience) or 100 μg/kg Zoledronic Acid (ZA) (Novartis) or 0.25 mg of Etanercept (Embrel) or 20U/kg of calcitonin (Calci)(Sigma). Clinical score was graded semi-quantitatively from 0 to 4 for each of the four following criteria: hunching, weight loss, diarrhea, and colon length as described,[3] Scores for each criterion were added to give an overall inflammation score for each mouse of 0–16. As control, C57Bl/6 mice were treated with zoledronic acid and calcitonin every day for 4 weeks.

DSS-induced colitis: C57BL/6 mice (8 weeks old; n = 4 per treatment group) were given 3 days of 3 % DSS in their drinking water and a final cycle of water for 4 days before sacrifice.

High resolution μCT

Fixed femora were scanned with high resolution μCT (Viva CT40, Scanco) (EcellFrance facility, Université Montpellier, France) as described in.[3]

Histological analysis

Femora were fixed in 4 % paraformaldehyde for 24 h at 4 °C, decalcified for 10 days in 10 % EDTA at 4 °C and incubated overnight in 30 % glucose solution. 7-μm bone sections were stained for TRAcP activity (leukocyte acid phosphatase kit, Sigma-Aldrich) according to the manufacturer's protocol. After hematoxylin staining, images were acquired on a light microscope (Carl Zeiss, Inc.). Colons were removed from the transferred Rag1-/- mice treated by ZA and Calci, fixed in Bouin's fixative, embedded in paraffin, sectioned at 5 μm and stained with H&E.

Primary osteoclast culture

Osteoclasts were differentiated from total murine BM cells as described previously,[42] collected from the culture plates using Accutase (Sigma-Aldrich) and sorted based on their multinucleation after Hoescht staining as previously described[25] for bulk RNAseq analysis. Inflammatory OCLs (i-OCLs) were generated as previously described[5].

RNA-sequencing on sorted osteoclasts

Total RNA was extracted with the RNeasy kit (Qiagen) and 100 ng RNA was processed for directional library preparation (Truseq stranded total RNA library kit, Illumina). Libraries were pooled and sequenced paired-ended for 2x75 cycles on a Nextseq500 sequencer (Illumina) to generate 30–40 million fragments per sample. Total RNA (100 ng) from 4 biological replicates (from 4 different mice) in each group was extracted from in vitro differentiated OCLs (after sorting according to their multinucleation as described in[25] with the RNeasy kit (Qiagen) and processed for directional library preparation (Truseq stranded total RNA library kit, Illumina). Libraries were pooled and sequenced paired-ended for 2 x 75 cycles on a Nextseq500 sequencer (Illumina) to generate 30–40 million fragments per sample. After quality controls, data analysis was performed with 2 different approaches. For the first one, reads were 'quasi' mapped on the reference mouse transcriptome (Gencode vM15) and quantified using the SALMON software with the mapping mode and standard settings.[43] Estimates of transcripts counts and their confidence intervals were computed using 1000 bootstraps to assess technical variance. Gene expression levels were computed by aggregating the transcript counts for each gene. Gene expression in biological replicates was then compared using a linear model as implemented in Sleuth[44] and a false discovery rate of 0.01. Lists of differentially expressed genes were annotated using Innate-DB and ShinnyGo web portals. For the second approach, raw RNAseq fastq reads were trimmed with Trimmomatic and aligned to the reference mouse transcriptome (Gencode mm10) using STAR (v. 2.6.1c)[45] on the National Institutes of Health high-performance computing Biowulf cluster. Gene-assignment and estimates counts of RNA reads were performed with HTseq.[46] Further analyses were performed with R software and gene expression in biological replicates (n = 4) was compared between the different conditions to identify differentially expressed genes using DESeq2[47] with the Wald test (FDR<0.01). Gene ontology (GO) pathway analyzes were performed using Goseq.[48] Both approaches gave equivalent results (not shown).

Gene expression analysis

Total RNA of sorted OCLs differentiated in vitro from BM of control and T cell-transferred *Rag1-/-* mice were extracted using TRIzol reagent following manufacturer's instructions. RT-qPCR was performed after reverse transcription (Superscript II, Life Technologies) as described previously using SYBR Green. List of primers: Mmp9 (5′-TGAGTCCGGCAGACAATCCT-3′; 5′-CGCCCTGGATCTCAGCAATA-3′), Mmp14 (5′–CCC TAG GCC TGG AAC ATT C-3′; 5′-TCT TTG TGG GTG ACC CTG ACT-3′), Ctsk (5′-CAGCAGAGGTGTGTACTATG-3′; 5′-GCGTTGTTCTTATTCCGAGC-3′), Samples of 3 biological replicates were run in triplicates and results were normalized to the reference gene 36B4 (5′-TCCAGGCTTTGGGCATCA-3′; 5′-CTTTATCAGCTGCACATCACTCAGA-3′) using the 2 − ΔCt method as described.[11]

Leukocyte Isolation, antibodies and flow cytometry

Single cell suspensions were prepared from spleen, Lamina Propria (LP) and BM as previously described[3] and were stained with different antibodies for FACS analysis (FACS canto, BD Biosciences) as indicated in the figures.

HSCs were analyzed after exclusion of lineage positive (Lin) cells using FITC-conjugated antibodies against CD3, B220, CD11b, Gr-1 and Ter-119, and after staining with PE-Cy7 Sca-1 and PE-c-kit. HSCs were indicated as Lin$^-$ Sca-1$^+$ c-kit$^+$ (LSK). Common myeloid progenitor (CMP), megacaryocyte-erythrocyte progenitor (MEP) and granulocyte-monocytes progenitors (GMP) were analyzed using Lin$^-$ Sca-1$^-$ c-kit^{high}, CD34 and CD16/CD32. For LSK proliferation, cells were fixed and stained with Ki-67.

Antibodies anti-CD3 (17A2), anti-CD11b (M1/70), anti-CD11c (HL3), anti-CD16/CD32 (2.4G2), anti-CD34 (RAM34), anti-c-kit (2B8), anti-Ly6C (AL-21), anti-Ly6G (1A8), anti-B220 (RA3-6B2), anti-MerTK (BB14-16) and anti-Ter119 (TER-119) were purchased from BD Biosciences (Le Pont De Claix, France). Purified anti-RANKL (IK22-5) was gift from CG. Mueller (CNRS UPR 3572, Strasbourg, France). Antibodies anti-CD45RB (C363,16A), Sca-1 (D7), anti-TNF-α (PA5-46945) and anti-Ki-67 (SOLA 15) were purchased from Thermo Fisher Scientific).

Colony forming assay

Sorted LSK cells from BM of control *Rag 1-/-* mice were suspended in methylcellulose medium and co-cultured with sorted OCLs from BM of colitic, control *Rag 1-/-* mice and inflammatory OCLs from BM of control mice or TNF-a KO mice and with or without control sorted BM CD45^{neg} cells considered as MSCs from control mice or TNF-a KO mice with or without anti-TNF-α (10 μg/ml) or mouse TNF-α (Peprotec, France), as indicated in the figures, to quantify clonogenic colony forming units in triplicate cultures (MethoCult GF M3434, Stem Cell Technologies). Colonies were scored after 10–14 days. CFU-G (granulocyte), M (macrophage), or GM (granulocyte–macrophage) colonies are referred to as CFU-GM.

Patients

PBMC and serum were isolated from freshly collected, heparinized peripheral blood of healthy voluntary donors and patients with Crohn's disease (CD) (Department of gastroenterology, CHU of Nancy, France). All the CD patients are naive without treatment at the time of blood collection. The protocol was approved by the local ethics committee of the Hospital Center of Nancy University and all patients and control subjects who were included in the study provided a signed informed consent. For the blood staining, mouse anti-human CD14, CD16, CD19, HLA-DR and CD66b were purchased from BD Biosciences for monocytes staining and the blood dendritic cell (DC) enumeration kit was purchased from Miltenyi Biotech.

Statistical analysis

All data were analyzed using Graph Pad Prism 8.0 software using an appropriate two tailed student's *t*-test with Bonferroni adjustment when comparing two groups. When more than two groups were compared two-way analysis of variance (ANOVA) was used. Statistical significance was considered at $p < 0.05$. Experimental values are presented as mean ± standard deviation (SD) of at least three biological replicas. Error bars for gene expression analysis of mice using RT-qPCR show the mean value with 95 % confidence interval. All experiments were repeated with a minimum of three biological replicates and at least two technical replicates.

Data availability

Sequencing reads have been deposited in European Nucleotide Archive (https://www.ebi.ac.uk/ena/) under accession number PRJEB41236. Other data will be available upon reasonable request.

CRediT authorship contribution statement

Maria-Bernadette Madel: Writing – original draft, Methodology, Formal analysis, Data curation. **Lidia Ibáñez:** Methodology, Formal analysis. **Thomas Ciucci:** Formal analysis. **Julia Halper:** Methodology, Data curation. **Antoine Boutin:** Methodology. **Ghada Beldi:** Methodology. **Alice C. Lavanant:** Methodology. **Henri-Jean Garchon:** Formal analysis, Data curation. **Matthieu Rouleau:** Writing – review & editing. **Christopher G. Mueller:** Writing – review & editing, Funding acquisition. **Laurent Peyrin-Biroulet:** Writing – review & editing, Funding acquisition. **David Moulin:** Writing – review & editing. **Claudine Blin-Wakkach:** Writing – review & editing, Writing – original draft, Funding acquisition, Conceptualization. **Abdelilah Wakkach:** Writing – review & editing, Writing – original draft, Supervision, Methodology, Funding acquisition, Formal analysis, Conceptualization.

Declaration of competing interest

The authors declare that they have no known competing financial interests or personal relationships that could have appeared to influence the work reported in this paper.

Acknowledgments

We are indebted to Pr G. Eberl for critical comments on the manuscript. This work was supported by the Agence Nationale de la Recherche (ANR-16-CE14-0030; ANR-19-CE14-0021-01; ANR-20-CE14-0037), the French Association François Aupetit, and the French government, managed by the ANR as part of the France 2030 Investment plan (ANR-23IAHU-0012) and the Investissement d'Avenir UCA^{JEDI} project (ANR-15-IDEX-01), and the Region Grand Est and the FEDER (for the FRCR Project TARGET (Translational research in Articular and Gastrointestinal Inflammatory Diseases in Grand Est). M-B M was supported by the Fondation pour la Recherche Médicale (FRM, ECO20160736019). J.H. was supported by the Société Française de Rhumatologie. We thank Adrien Mahler for technical help and Majlinda Topi for animal care. We acknowledge the Genomic Facility of the UFR Simone Veil, (Université Versailles-Saint-Quentin, France) for the RNA sequencing, the IRCAN animal core facility (Nice, France) and the preclinical platform of ECELLFRANCE for microCT analysis (IRMB, Montpellier, France). This work utilized the computational resources of the NIH-HPC-Biowulf cluster (http://hpc.nih.gov).

Appendix A. Supplementary data

Supplementary data to this article can be found online at https://doi.org/10.1016/j.mucimm.2024.09.005.

References

1. Targownik LE, Bernstein CN, Leslie WD. Risk factors and management of osteoporosis in inflammatory bowel disease. *Curr Opin Gastroenterol*. 2014;30:168–174.
2. Tilg H, Moschen AR, Kaser A, Pines A, Dotan I. Gut, inflammation and osteoporosis: basic and clinical concepts. *Gut*. 2008;57:684–694.
3. Ciucci T, et al. Bone marrow Th17 TNFα cells induce osteoclast differentiation, and link bone destruction to IBD. *Gut*. 2015;64:1072–1081.
4. Madel M-B, et al. Immune function and diversity of osteoclasts in normal and pathological conditions. *Front Immunol*. 2019;10.
5. Ibáñez L, et al. Inflammatory osteoclasts prime TNFα-producing CD4(+) T cells and express CX3 CR1. *J Bone Miner Res*. 2016. https://doi.org/10.1002/jbmr.2868.
6. Grassi F, et al. T cell suppression by osteoclasts in vitro. *J Cell Physiol*. 2011;226:982–990.
7. Kiesel JR, Buchwald ZS, Aurora R. Cross-presentation by osteoclasts induces FoxP3 in CD8+ T cells. *J Immunol*. 2009;182:5477–5487.
8. Lapid K, *et al.* Egress and mobilization of hematopoietic stem and progenitor cells: a dynamic multi-facet process. In *StemBook* (Harvard Stem Cell Institute, Cambridge (MA), 2008).at <http://www.ncbi.nlm.nih.gov/books/NBK133261/>.
9. Lévesque J-P, Helwani FM, Winkler IG. The endosteal 'osteoblastic' niche and its role in hematopoietic stem cell homing and mobilization. *Leukemia*. 2010;24:1979–1992.
10. Morrison SJ, Scadden DT. The bone marrow niche for haematopoietic stem cells. *Nature*. 2014;505:327–334.
11. Mansour A, et al. Osteoclasts promote the formation of hematopoietic stem cell niches in the bone marrow. *J Exp Med*. 2012;209:537–549.
12. Mansour A, et al. Osteoclast activity modulates B-cell development in the bone marrow. *Cell Res*. 2011;21:1102–1115.
13. Mansour A, Wakkach A, Blin-Wakkach C. Role of osteoclasts in the hematopoietic stem cell niche formation. *Cell Cycle*. 2012;11:2045–2046.
14. Kollet O, et al. Osteoclasts degrade endosteal components and promote mobilization of hematopoietic progenitor cells. *Nat Med*. 2006;12:657–664.
15. Lymperi S, Ersek A, Ferraro F, Dazzi F, Horwood NJ. Inhibition of osteoclast function reduces hematopoietic stem cell numbers in vivo. *Blood*. 2011;117:1540–1549.
16. Oduro KA, et al. Myeloid skewing in murine autoimmune arthritis occurs in hematopoietic stem and primitive progenitor cells. *Blood*. 2012;120:2203–2213.
17. Griseri T, McKenzie BS, Schiering C, Powrie F. Dysregulated hematopoietic stem and progenitor cell activity promotes interleukin-23-driven chronic intestinal inflammation. *Immunity*. 2012;37:1116–1129.
18. Sezaki M, et al. Hematopoietic stem and progenitor cells integrate microbial signals to promote post-inflammation gut tissue repair. *EMBO J*. 2022;41:e110712.
19. Blin-Wakkach C, Rouleau M, Wakkach A. Roles of osteoclasts in the control of medullary hematopoietic niches. *Arch Biochem Biophys*. 2014. https://doi.org/10.1016/j.abb.2014.06.032.
20. Izcue A, et al. Interleukin-23 restrains regulatory T cell activity to drive T cell-dependent colitis. *Immunity*. 2008;28:559–570.
21. Powrie F, Carlino J, Leach MW, Mauze S, Coffman RL. A critical role for transforming growth factor-beta but not interleukin 4 in the suppression of T helper type 1-mediated colitis by CD45RB(low) CD4+ T cells. *J Exp Med*. 1996;183:2669–2674.
22. Wakkach A, Augier S, Breittmayer J-P, Blin-Wakkach C, Carle GF. Characterization of IL-10-secreting T cells derived from regulatory CD4+CD25+ cells by the TIRC7 surface marker. *J Immunol*. 2008;180:6054–6063.
23. Russell RGG, Watts NB, Ebetino FH, Rogers MJ. Mechanisms of action of bisphosphonates: similarities and differences and their potential influence on clinical efficacy. *Osteoporos Int*. 2008;19:733–759.
24. Tomimori Y, et al. Evaluation of pharmaceuticals with a novel 50-hour animal model of bone loss. *J Bone Miner Res*. 2009;24:1194–1205.
25. Madel M-B, Ibáñez L, Rouleau M, Wakkach A, Blin-Wakkach C. A novel reliable and efficient procedure for purification of mature osteoclasts allowing functional assays in mouse cells. *Front Immunol*. 2018;9:2567.
26. Kollet O, Dar A, Lapidot T. The multiple roles of osteoclasts in host defense: bone remodeling and hematopoietic stem cell mobilization. *Annu Rev Immunol*. 2007;25:51–69.

27. Saw S, Weiss A, Khokha R, Waterhouse PD. Metalloproteases: on the watch in the hematopoietic niche. *Trends Immunol*. 2019;40:1053–1070.
28. Christgau S, et al. Serum CrossLaps for monitoring the response in individuals undergoing antiresorptive therapy. *Bone*. 2000;26:505–511.
29. Hanai H, et al. Adsorptive depletion of elevated proinflammatory CD14+CD16+DR ++ monocytes in patients with inflammatory bowel disease. *Am J Gastroenterol*. 2008;103:1210–1216.
30. Koch S, Kucharzik T, Heidemann J, Nusrat A, Luegering A. Investigating the role of proinflammatory CD16+ monocytes in the pathogenesis of inflammatory bowel disease. *Clin Exp Immunol*. 2010;161:332–341.
31. Hoggatt J, Pelus LM. Mobilization of hematopoietic stem cells from the bone marrow niche to the blood compartment. *Stem Cell Res Ther*. 2011;2:13.
32. Hoggatt J, et al. Rapid mobilization reveals a highly engraftable hematopoietic stem cell. *Cell*. 2018;172:191–204.e10.
33. Zhu L, et al. Osteoclast-mediated bone resorption is controlled by a compensatory network of secreted and membrane-tethered metalloproteinases. *Sci Transl Med*. 2020;12.
34. Kleyer A, et al. Bone loss before the clinical onset of rheumatoid arthritis in subjects with anticitrullinated protein antibodies. *Ann Rheum Dis*. 2014;73:854–860.
35. Kocijan R, Harre U, Schett G. ACPA and bone loss in rheumatoid arthritis. *Curr Rheumatol Rep*. 2013;15:366.
36. Peek CT, et al. Intestinal inflammation promotes MDL-1+ osteoclast precursor expansion to trigger osteoclastogenesis and bone loss. *Cell Mol Gastroenterol Hepatol*. 2022;14:731–750.
37. Palmen MJ, Dijkstra CD, van der Ende MB, Peña AS, van Rees EP. Anti-CD11b/CD18 antibodies reduce inflammation in acute colitis in rats. *Clin Exp Immunol*. 1995;101: 351–356.
38. Yokoyama Y, et al. Efficacy of granulocyte and monocyte adsorptive apheresis in patients with inflammatory bowel disease showing lost response to infliximab. *J Crohns Colitis*. 2020. https://doi.org/10.1093/ecco-jcc/jjaa051.
39. Hu Y, et al. Bone loss prevention of bisphosphonates in patients with inflammatory bowel disease: a systematic review and meta-analysis. *Can J Gastroenterol Hepatol*. 2017;2017:2736547.
40. Veltman JD, et al. Zoledronic acid impairs myeloid differentiation to tumour-associated macrophages in mesothelioma. *Br J Cancer*. 2010;103:629–641.
41. Wolf AM, et al. The effect of zoledronic acid on the function and differentiation of myeloid cells. *Haematologica*. 2006;91:1165–1171.
42. Madel M-B, et al. Dissecting the phenotypic and functional heterogeneity of mouse inflammatory osteoclasts by the expression of Cx3cr1. *Elife*. 2020;9.
43. Patro R, Duggal G, Love MI, Irizarry RA, Kingsford C. Salmon provides fast and bias-aware quantification of transcript expression. *Nat Methods*. 2017;14:417–419.
44. Pimentel H, Bray NL, Puente S, Melsted P, Pachter L. Differential analysis of RNA-seq incorporating quantification uncertainty. *Nat Methods*. 2017;14:687–690.
45. Dobin A, et al. STAR: ultrafast universal RNA-seq aligner. *Bioinformatics*. 2013;29: 15–21.
46. Anders S, Pyl PT, Huber W. HTSeq–a Python framework to work with high-throughput sequencing data. *Bioinformatics*. 2015;31:166–169.
47. Love MI, Huber W, Anders S. Moderated estimation of fold change and dispersion for RNA-seq data with DESeq2. *Genome Biol*. 2014;15:550.
48. Young MD, Wakefield MJ, Smyth GK, Oshlack A. Gene ontology analysis for RNA-seq: accounting for selection bias. *Genome Biol*. 2010;11:R14.